# Control Barrier Function-Based Force Constrained Safety Compliance Control for Manipulator

Haiyan Liang[1], Xinming Wang[1]*, Jianliang Mao[2], Jun Yang[3]
1. The Key Laboratory of Measurement and Control of CSE, Ministry of Education,
School of Automation, Southeast University, Nanjing 210096, China.
2. College of Automation Engineering, Shanghai University of Electric Power, Shanghai 200090, PR China
3. Department of Aeronautical and Automotive Engineering, Loughborough University Loughborough LE11 3TU, UK
lhy_seu@seu.edu.cn, wxm_seu@seu.edu.cn, jl_mao@shiep.edu.cn, j.yang3@lboro.ac.uk (corresponding author*)

2023 28th International Conference on Automation and Computing (ICAC) | 979-8-3503-3585-9/23/$31.00 ©2023 IEEE | DOI: 10.1109/ICAC57885.2023.10275266

***Abstract*—In this paper, a safety-critical compliance control with force constraint is proposed for the interaction task of a manipulator in the Cartesian space. Different from the conventional impedance control approach, the interaction force constraint is considered and interpreted by designing a new Force Constrained Control Barrier Function (FCCBF) with exploiting the environment model. By formulating and solving a quadratic programming with modifying the baseline impedance controller under the FCCBF constraint, the proposed controller can not only make manipulator's interaction process satisfy expected compliance without exceeding permissible contact force range, but can also improve the dynamic characteristics of the system by eliminating force overshooting phenomena. Furthermore, with using the technique of nonlinear disturbance observer, a force sensor-less FCCBF approach is also provided, where the contact force is treated as an external disturbance. Finally, the effectiveness of the proposed algorithms is verified by both simulations and experimental tests on a 6 degree-of-freedom manipulator.**

***Keywords—force safety control, impedance control, control barrier function, manipulator***

## I. INTRODUCTION

With the technical development of manufacturing industry, manipulators have been used intensively. In conventional manipulating tasks, e.g., simple assembly and handling, the manipulator operates in single mode with fixed manners, barely considering the impact of contact forces with objects. However, in complex interactive tasks like surface grinding and polishing [1], contact forces must be precisely controlled to achieve maximal manufacturing precision and admissible safety guarantee. Additionally, for Human-Machine Interaction (HMI) tasks, in which the robotic arm directly contacts with humans, excessive contact force may cause injures or even casualties [2]. Therefore, safety and compliance must be integrated into the control design of the manipulator.

Traditional compliance control strategies can be divided into passive compliance control and active compliance control. The passive compliance control is mainly achieved in a mechanical way like implementing some damping spring elements [3]. The latter, active compliance control, consists of direct force control and indirect force control, represented by force/position hybrid control [4][5] and impedance control [6][7] respectively. The force/position hybrid control in [4][5] usually achieves compliant force control task by dividing the control objectives into position control and force control task spaces. Impedance control, on the other hand, considers motion and force as an unity, revealing a better approach by controlling the force-position relationship [8]. Compared with force/position hybrid control, impedance control is more robust to uncertainty and disturbance, and prone to obtain adjustable dynamic response with higher control bandwidth, resulting in a broader applications in robot interactive tasks [9]-[11]. To be specific, in [9], an improved impedance control method with variable damping and force feedback enhancement is applied to a surgical robot, and the suppression effect of this method on hand tremor is verified by virtual experiments. In [10], a position-based impedance control method is designed to realize the handling task of a mobile dual-arm robot, in which the joint torque interface is not necessary by correcting the target position according to the impedance algorithm. Additionally, for high-precision contact force control scenarios, the combination of adaptive control with impedance control is used by establishing adaptive parameter update methods through kinematic and dynamic models [11]. Although the above methods have made improvements in application-specific scenarios, they do not consider strict contact force constraints, which means that excessive contact force may violate some specified safety regions induced by external environment even if the compliance is ensured by impedance control algorithm. Therefore, it is imperative to study an impedance control method considering strict force constraints.

In terms of advanced control approaches achieving safety guarantee for nonlinear systems, control barrier function (CBF) has been increasingly studied in recent years since it provides an effective way to guarantee the complex specified safety constraints [12]-[14]. In [15], CBF is used for obstacle avoidance and safe distance maintenance for the control of multi-mobile robots by designing a suitable safety set. Similarly, collision avoidance in cartesian space can also be achieved by designing a distance-constraint CBF for robotic arms [16]. However, the above safety guarantees of robotics arms are interpreted by position, which may fail to specify the strict force constraint and require high computational accuracy if the contact environment model is with high stiffness.

In this paper, a force-constrained safety compliance control (FCSCC) strategy based on a new control barrier function is designed. Firstly, we establish the dynamic model

of the 6-DOF manipulator and then the impedance controller of the manipulator is designed as the benchmark controller. The environment model is modeled as a rigid body model inspiring from [17], in which the contact force is linear to the environmental deformation when the deformation is positive, and remains zero otherwise. With this in mind, the Force Constrained Control Barrier Function (FCCBF) is designed to constrain the contact force if the end-effector is approaching the environment border. Afterwards, by considering the FCCBF constraint, the proposed control policy is formulated as a quadratic programming with modifying the benchmark controller in a minimum invasion way. The rigorous theoretical analysis of strict force constraint is presented. In the case of lacking the force sensors, an observer-based force sensor-less force constrained compliance control approach is provided by treating the contact force as an unknown external disturbance. Through the simulations and experimental tests of a 6-DOF manipulator, it can be verified that both the proposed controllers not only increase the compliance but also strictly limit the contact force within the safety region.

The subsequent sections of this paper is arranged as follows. Section II introduces the background knowledge of CBF and the dynamic model of the manipulator system. Section III gives main results of proposed control approach. Section IV presents the further discussion on NDOB-based force sensor-less FCSCC. Simulation results are presented in Section V. Finally, the conclusion is in Section VI.

**Notation**: Define $R$ as the real numbers, where subscripts are added to name vector or matrix space. Let $C^r$ to be the r-th continuous differentiable function set. If a continuous function $\alpha:[0,e)\to[0,\infty)$ for some $e>0$ is strictly monotonically increasing and $\alpha(0)=0, \lim_{r\to\infty}\alpha(r)=\infty$, it is said to be class $K_\infty$, and if a continuous function $\alpha:(-w,e)\to(-\infty,\infty)$ for some $w,e>0$ is strictly monotonically increasing and $\alpha(0)=0$, it is said to be extended class $K_\infty$.

## II. Preliminaries and Problem Formulation

### A. Control Barrier Function

Consider a nonlinear affine control system like:

$$\dot{x}=f(x)+g(x)u, \tag{1}$$

with state $x\in R^n$, input $u\in R^m$, and functions $f:R^n\to R^n$, $g:R^n\to R^{n\times m}$ assumed to be locally Lipschitz continuous on $R^n$.

We assume a set $\mathrm{C}\subset R^n$ as a superlevel set of a continuous differentiable function $h(x):R^n\to R$, and the boundary ∂C and interior Int(C) of the set are defined as follows:

$$\begin{cases} \mathrm{C}=\{x\in R^n: h(x)\ge 0\}, \\ \partial\mathrm{C}=\{x\in R^n: h(x)=0\}, \\ \mathrm{Int}(\mathrm{C})=\{x\in R^n: h(x)>0\}. \end{cases} \tag{2}$$

For any initial condition $x_0:=x(t_0)\in R^n$, there exists a maximum time interval $\mathrm{T}(x_0)=[0,t_{\max})$ such that $x(t)$ is the unique solution to (1) on $\mathrm{T}(x_0)$. Then, the set C is a forward invariant set if for any initial states $x_0\in\mathrm{C}$, $x(t)\in\mathrm{C}$ for all $t\in\mathrm{T}(x_0)$. Here we define the concept of safety in this situation as forward invariance of a set in the state space. In such case, the system (1) is *safe* with respect to the set C, and C is called a *safe set*.

*Definition 1 (Control Barrier Functions)* [14]: Given a set $\mathrm{C}\subset R^n$ defined by (2), the function $h(x)$ with $\frac{\partial h}{\partial x}(x)\neq 0$, if $h(x)=0$ is called as the CBF if there exists an extended class $K_\infty$ function $\alpha$, for all $x(t)\in\mathrm{C}$:

$$\sup_{u\in R^m}[L_f h(x)+L_g h(x)u]\ge -\alpha(h(x)), \tag{3}$$

where $L_f h(x)=\frac{\partial h}{\partial x}(x)f(x)$, $L_g h(x)=\frac{\partial h}{\partial x}(x)g(x)$ are in the form of standard Lie derivative. Given a valid CBF $h(x):R^n\to R$, if the initial states of system satisfy $x(0)\in\mathrm{C}$, then any Lipschitz continuous controller $u(t)$ belonging to $S_{cbf}(x)=\{u\in R^m\mid: L_f h(x)+L_g h(x)u+\alpha(h(x))\ge 0\}$ renders the system (1) safe.

It should be highlighted that the relative degree of the system is assumed to be one, which means that the first order time-derivative of the barrier function is related to the system control input. However, for manipulator system, the relative-degree is not exactly to be one [14].

*Definition 2 (Exponential Control Barrier Functions (ECBFs))* [18]: For high-relative-degree safety constraint system, $h(x)\in C^r$ with a relative degree $r\ge 2$, is an Exponential Control Barrier Function (ECBF) if there is a row vector $K_\alpha\in R^r$ such that:

$$\sup_{u\in R^m}\underbrace{L_f^r h(x)+L_g L_f^{r-1}h(x)u}_{h^r(x,u)}\ge -K_\alpha\beta_b(x), \tag{4}$$

where $\beta_b(x):=\left[h(x),\dot{h}(x),\ddot{h}(x),...,h^{r-1}(x)\right]^T=\left[h(x),L_f h(x),L_f^2 h(x),...,L_f^{r-1}h(x)\right]^T$. The functions $\varphi_k(x(t))$ for $k=0,1,...,r$ are defined recursively as $\varphi_0(x(t))=h(x(t))$, $\varphi_k(x(t))=\left(\frac{d}{dt}+\lambda_k\right)\varphi_{k-1}$.

Similarly, given a valid ECBF $h(x):R^n\to R$, it was proven in [18] if $\varphi_k(x(0))>0$ for $k=0,1,...,r$, then any Lipschitz continuous controller $u(t)$ belonging to $S_{ecbf}(x)=\{u\in R^m\mid: L_f^r h(x)+L_g L_f^{r-1}h(x)u+K_\alpha\beta_b(x)\ge 0\}$ renders the system (1) safe.

### B. 6-DOF Manipulator Model

A rigid robotic arm system dynamic model can be given in joint space as follows:

$$M(q)\ddot{q}+C(q,\dot{q})\dot{q}+G(q)=\tau-\tau_e, \tag{5}$$

where $q\in R^n$ is the generalized coordinates of the manipulator's joint positions, $M(q)\in R^{n\times n}$ represents a general inertial matrix. $C(q,\dot{q})\in R^{n\times n}$ means the effect of centrifugal force and Coriolis, and $G(q)\in R^n$ describes the gravity torque of the system. The pose of the end-effector is represented by $\zeta\in R^6$ with $\dot{\zeta}=J(q)\dot{q}$ and $\tau_e=J^T(q)F_e$, where $J(q)$ denotes the Jacobian matrix. Since the interactions are usually described in the Cartesian space, the robot system can be rewritten as follows:

$$M_\zeta\ddot{\zeta}+C_\zeta\dot{\zeta}+G_\zeta=\tau-J^T F_e, \tag{6}$$

where $M_\zeta = M(q)J^{-1}(q), C_\zeta = -M(q)J^{-1}(q)\dot{J}(q)J^{-1}(q) + C(q,\dot{q})J^{-1}(q),\ G_\zeta = G(q).$

For a full-drive robotic arm, $M_\zeta \in R^{6\times6}$ , $C_\zeta \in R^{6\times6}$ , $G_\zeta \in R^6$ . $F_e \in R^6$ represents the contact force/torque of the end-effector, and $\tau \in R^6$ is the driving torque.

Defining $u = \tau$ , and $x_1 = \zeta$ , $x_2 = \dot{\zeta}$ , then system (6) can be rewritten as following form:

$$\dot{x} = A(x) + B(x)u, \tag{7}$$

where $A(x) = \left[x_2, -M_\zeta^{-1}(C_\zeta x_2 + G_\zeta + J^T F_e)\right]^T$ , $B(x) = \left[0, M_\zeta^{-1}\right]^T$ .

***Assumption 1***: The end-effector of the robotic arm can avoid the singularity position through trajectory planning, so the Jacobian matrix $J(q)$ of the robotic arm has full rank.

According to assumption 1, matrix $M_\zeta$ is invertible since $M(q)$ and $J(q)$ are invertible, $M_\zeta{}^{-1} = J(q)M^{-1}(q)$.

### C. Environment Model

Denoting a transformation matrix $R \in R^{6\times6}$ between the compliance and the operational coordinates, the environment model from [17] can be constructed as a friction-free rigid model described as follows:

$$\begin{cases} F_e^c = K_{env}(\zeta^c - \zeta_e^c),\ \zeta^c \geq \zeta_e^c, \\ F_e^c = 0,\ \zeta^c < \zeta_e^c, \end{cases} \tag{8}$$

where $\zeta^c = R^T\zeta$ , $F_e^c = R^T F_e$ and $K_{env} \in R^{6\times6}$ is a diagonal environmental stiffness matrix and $\zeta_e^c \in R^6$ is the environmental position that starts to generate contact with the end-effector of the robotic arm.

***Control Objective***: The goal of this paper is to design a force-constrained safety-critical compliance controller for manipulators working within the environment constraint specified by (8).

## III. Main Results

In this section, the baseline impedance controller is firstly introduced. Then we design the contact force constraint in the Cartesian space and present the formulation of the FCCBF. Finally, the force-constrained safety compliance controller is derived.

### A. Design of Impedance Controller

In this study, the impedance controller is selected as the nominal controller to achieve the position and contact force control. The essence of impedance control is to establish the relationship between force and position errors:

$$F_d - F_e = M_d(\ddot{\zeta} - \ddot{\zeta}_{ref}) + D_d(\dot{\zeta} - \dot{\zeta}_{ref}) + K_d(\zeta - \zeta_{ref}), \tag{9}$$

where $F_d \in R^6$ is the expected value of the spatial force/torque of cartesian, $M_d \in R^{6\times6}$ , $D_d \in R^{6\times6}$ and $K_d \in R^{6\times6}$ are the expected compliant diagonal parameter matrix of the robotic arm operation space, and $\zeta_{ref}, \dot{\zeta}_{ref}, \ddot{\zeta}_{ref}$ are the reference motion information of the end-effector which are given by trajectory planning.

Combining (6) and (9), the analytical expression of the impedance controller is obtained:

$$\begin{aligned} \gamma^d = {} & M_\xi M_d{}^{-1}(F_d - D_d(\dot{\zeta} - \dot{\zeta}_{ref}) - K_d(\zeta - \zeta_{ref})) \\ & + M_\xi \ddot{\zeta}_{ref} + C_\xi \dot{\zeta} + G_\xi + (J^T - M_\xi M_d{}^{-1})F_e. \end{aligned} \tag{10}$$

### B. Force-Constrained Safety Compliance Controller Design

This part we give detailed steps to construct a force-constrained safety compliance controller. Using the baseline impedance controller given in part *A*, we can obtain basic compliance of the interaction, and then a FCCBF is supposed to be designed to realize safety.

According to the environment model formulated in (8), the contact force remains zero until actual deformation happens, and is non-negative. Then we only need to restrain the upper boundary of the interact force. The maximum safety value of contact force can be noted as a positive constant $F_{e\max}^c$ , and the safety condition is:

$$F_e^c \leq F_{e\max}^c. \tag{11}$$

Combining (8) and (11) , we define a continuously differentiable function $h(x): R^n \to R$ as:

$$h(x) = F_{e\max}^c - K_{env}(\zeta^c - \zeta_e^c),\ \zeta^c \geq \zeta_e^c. \tag{12}$$

Taking (12) into consideration, the relative-degree of the system is obviously to be two. Inspired by the design of ECBF, we define a set of functions $\varphi_0(x(t)), \varphi_1(x(t)), \varphi_2(x(t))$ as:

$$\begin{cases} \varphi_0(x(t)) = h(x(t)), \\ \varphi_1(x(t)) = \left(\frac{\mathrm{d}}{\mathrm{dt}} + \lambda_1\right)\varphi_0, \\ \varphi_2(x(t)) = \left(\frac{\mathrm{d}}{\mathrm{dt}} + \lambda_2\right)\varphi_1, \end{cases} \tag{13}$$

where $\lambda_1, \lambda_2$ are positive constants, and then the following superlevel sets can be given as:

$$\begin{cases} C_0 = \{x \in R^n \mid \varphi_0(x) \geq 0\}, \\ C_1 = \{x \in R^n \mid \varphi_1(x) \geq 0\}. \end{cases} \tag{14}$$

According to the descriptions above, we can give the following definition of FCCBF.

*Definition 3:* Consider the system (7) and sets defined in (14). The function $h(x)$ in (12) is a FCCBF of relative degree two, if there exists constants $a > 0$ and $b > 0$ subject to

$$\sup_{u \in R^m} \left\{ \begin{matrix} -K_{env}\left[M_\zeta{}^{-1}\left(u - J^T F_e - C_\zeta\dot{\zeta} - G_\zeta\right)\right] \\ +a\left[F_{e\max}^c - K_{env}(\zeta - \zeta_e)\right] - bK_{env}\dot{\zeta} \end{matrix} \right\} \geq 0, \tag{15}$$

for all $x(t) \in C_{mix} := C_0 \bigcap C_1$ . The adjustable constants $a, b$ can be designed by pole assignment method to make the root of $p(\lambda) = \lambda^2 + a\lambda + b$ are all negative reals $-\lambda_1, -\lambda_2$ . Then we can conclude the following theorem to guarantee the safety of system in (7) described by set $C_{mix}$.

*Theorem 1:* Given a valid FCCBF $h(x): R^n \to R$ , if the initial states of system satisfy $\varphi_0(x(0)) \in C_{mix}$, $\varphi_1(x(0)) \in C_{mix}$ , then any Lipschitz continuous controller $u(t)$ belonging to

$S_{fccbf}(x)=\{u\in R^m \mid -K_{env}\left[M_\zeta^{-1}\left(u-J^T F_e-C_\zeta\dot{\zeta}-G_\zeta\right)\right]$ $+a\left[F_{e\max}^c-K_{env}(\zeta-\zeta_e)\right]-bK_{env}\dot{\zeta}\geq 0\}$ renders the set $C_{mix}$ forward invariant.

*Proof*: Firstly, it can be obtained that $\varphi_2\geq 0$ since there exists a Lipschitz continuous controller $u(t)\in S_{fccbf}$, then we can get $\dot{\varphi}_1=-\lambda_2\varphi_1+\varphi_2$ from (13) such that the set $C_1$ is forward invariant with $\varphi_1(0)>0$. Similarly, the set $C_0$ is also forward invariant with $\varphi_0(0)>0$ by the guarantee of $\varphi_1\geq 0$. Therefore, the forward invariance of set $C_{mix}$ can be guaranteed, and thus the strict safety constraint is achieved. This completes the proof. ■

In order to ensure the nominal control objective, the proposed strategy needs to modify the nominal controller (10) as little as possible. With this in mind, the following quadratic programming (QP) problem is used to generate the Lipschitz continuous controller $\gamma(x)$:

$$\gamma(x,t)=\arg\min_{u\in R^m}\frac{1}{2}\left\|u-\gamma^d(x,t)\right\|_2^2,$$
$$s.t.\ \ddot{h}(x,u)+a\left[F_{e\max}-K_{env}(\zeta-\zeta_e)\right]-bK_{env}\dot{\zeta}\geq 0. \quad (16)$$

The overall diagram of the control system is shown in Fig. 1.

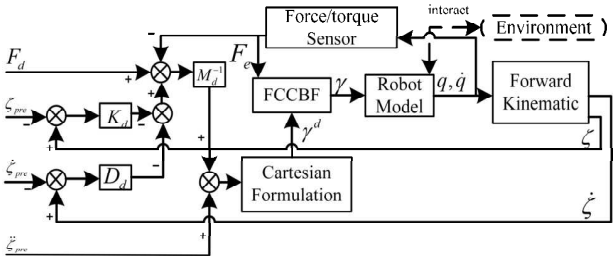


Fig. 1. Block Diagram of Safety Force Control Based on FCCBF

## IV. Further Discussion on NDOB-Based Force Sensorless FCSCC

As shown in Fig. 1, the contact force is measured by a six-dimensional force/torque sensor, which some robotic arms may not be equipped with. Taking this into consideration, a nonlinear disturbance observer (NDOB) is designed as a replacement of force/torque sensor to estimate the contact force acting on the end-effector. For nonlinear dynamic system (5), considering $\tau_e$ as the disturbance, the following NDOB can be developed inspiring from [19]:

$$\begin{cases}\dot{z}=L(q,\dot{q})(C(q,\dot{q})\dot{q}+G(q)-\tau-p(q,\dot{q}))-L(q,\dot{q})z,\\ \hat{\tau}_e=z+p(q,\dot{q}),\end{cases} \quad (17)$$

where $z\in R^n$ is the internal state vector of the NDOB, $L(q,\dot{q})\in R^{n\times n}$ and $p(q,\dot{q})\in R^n$ are the gain matrix and the auxiliary vector of the NDOB respectively, and $\hat{\tau}_e\in R^n$ is the estimated external torque vector in the joint space. It is clear that $\hat{\tau}_e$ can be converted into the estimation of the contact force $\hat{F}_e$ by

$$\hat{F}_e=J^{-T}(q)\hat{\tau}_e. \quad (18)$$

In order to guarantee the stability, we assume that the time derivatives of $\tau_e$ and $\dot{q}$ are bounded respectively by unknown limits, and thus the external torque can be estimated by NDOB (17) with $p=\Lambda\dot{q}$ and $L=\Lambda M^{-1}(q)$, where $\Lambda$ is a diagonal positive definite matrix. It has been proven in [20] that larger (smaller) values of $\Lambda$ correspond to faster (slower) convergence at the expense of larger (smaller) overshoot. Then the control diagram in Fig. 1 can be revised to a sensorless form as shown in Fig. 2:

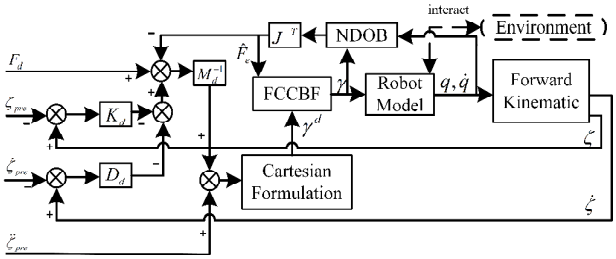


Fig. 2. Block Diagram of FCSCC combined with NDOB

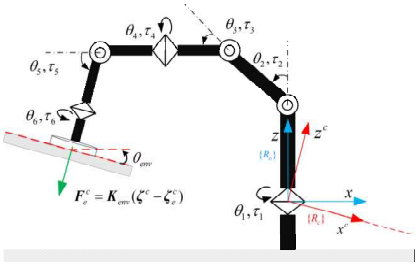

Fig. 3. 6-DOF manipulator contact task scenario

## V. Simulation Results

In this section, a MATLAB simulation program is designed to verify the effectiveness of the proposed algorithm. By using MATLAB Robotics Toolbox, we create a 6-DOF gravity-compensated robotic arm dynamic model as (7) with its main parameters shown in TABLE I. , in which $L_i,(i=1,2,...6)$ represents link $i$ on the robotic arm, $l_d$ is the length of the link, $l_a$ is the displacement and $\alpha$ indicates the reversing

TABLE I. 6-DOF Robotic Arm Simulation Model Parameters

| | $l_d$(m) | $l_a$(m) | $\alpha$(°) | $q_{lim}$(°) | $g_e$ | $m$(kg) | $\Gamma(\times10^{-2}\text{kg}\cdot\text{m}^2)$ |
|---|---|---|---|---|---|---|---|
| $L_1$ | 0 | 0 | 90° | [−160°,160°] | -62.6 | 0 | {0,35,0,0,0,0} |
| $L_2$ | 0 | 0.43 | 0 | [−45°,225°] | 107.8 | 17.4 | {13,52,54,0,0,0} |
| $L_3$ | 0.15 | 0.02 | −90° | [−225°,45°] | -53.7 | 4.8 | {6.6,8.6,1.3,0,0,0} |
| $L_4$ | 0.43 | 0 | 90° | [−110°,170°] | 76.1 | 0.8 | {0.2,0.1,0.2,0,0,0} |
| $L_5$ | 0 | 0 | −90° | [−100°,100°] | 71.9 | 0.3 | {0.03,0,04,0,03,0,0,0} |
| $L_6$ | 0 | 0 | 0 | [−266°,266°] | 76.7 | 0.1 | {0.02,0.02,0,0,0,0} |

angle of the link, $q_{lim}$ represents the range of joint angles, $g_e$ represents the reduction ratio of the motor, $m$ is the mass of the link, and $\Gamma = \{l_{xx}, l_{yy}, l_{zz}, l_{xy}, l_{yz}, l_{xz}\}$ is the parameter set of the inertia of link $i$ (under the coordinate system).

In this simulation, we design the contact task scenario as shown in Fig. 3, which includes a fixed plane as environment. The angle between the rigid surface and the horizontal plane is $\theta = 0^\circ$ with the rotation matrix $R = I_{6\times6}$, and the end-effector applies vertical force to the surface. Therefore, we only pay attention to the contact force and compliant position and the controller output in the Z-axis of the world coordinate. The expected value of the contact force is set to $F_d^c = [0,0,50,0,0,0]^T$. The position of the surface is fixed to $\zeta_e^c = [-0.43,-0.15,-0.2,0,0,0]^T$. The initial value of expected position, velocity and acceleration of the manipulator in Cartesian space are $\zeta_{ref} = [-0.43,-0.15,-0.4,0,0,0]^T$, $\dot{\zeta}_{ref} = \boldsymbol{0}_{6\times1}$ and $\ddot{\zeta}_{ref} = \boldsymbol{0}_{6\times1}$.

The parameters of impedance controller are set as $M_d = 2\times I_{6\times6}, D_d = 10\times I_{6\times6}, K_d = 200\times I_{6\times6}$, and the initial value of the Z-axis environment stiffness is $K_{env}^{c_z} = 250$. During the interaction, force shocks may occur if the parameters $M_d, D_d, K_d$ cannot make the closed-loop system in an overdamped mode. In order to verify the effectiveness of the contact force safety constraint and force shock suppression, the FCSCC with a safety boundary $F_{e\max}^c = 50N$ is compared with the traditional impedance control approach. The parameters of the constraints of FCCBF are $a = 300, b = 35$. Additionally, according to Section IV, we design a NDOB as (17), and obtain the estimation of contact force $\hat{F}_e$ by (18). The NDOB parameter matrix $\Lambda$ is set as $\Lambda = 100\text{diag}([1;2.5;3;1;1;1])$, where $\text{diag}(\cdot)$ is a diagonal matrix. The initial value of $z$ is set as $z_0 = [0,0,0,0,0,0]^T$.

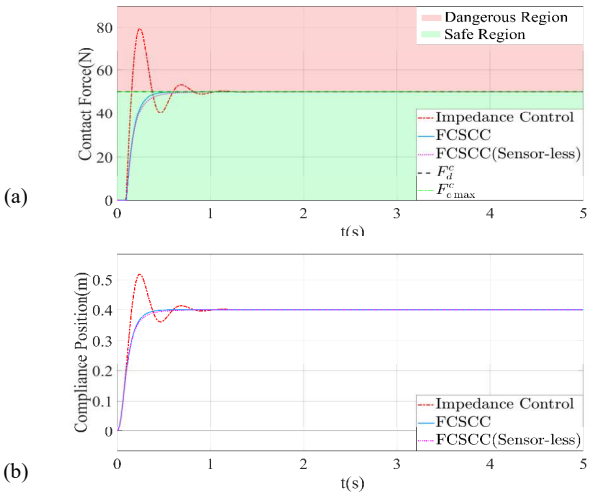


Fig. 4. Contact forces and compliance positions during interaction with the environment ($K_{env}^{c_z} = 250$) under different strategies: (a) trajectories of contact forces; (b) trajectories of compliance positions.

Fig. 4 (a) shows that the actual value of the contact force can be constrained within the boundary, and finally converges to the expected value. Meanwhile, the position also compliantly converges to reference value in Fig. 4 (b), showing that the proposed algorithm can completely limit the unsafe variation of contact force under the premise of ensuring the effect of impedance control. Besides, comparing force

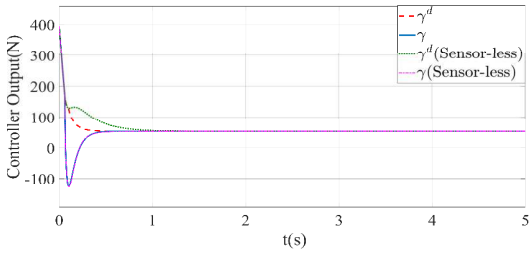


Fig. 5. Modified outputs $\gamma$ and baseline outputs $\gamma^d$ of sensor-based FCSCC and NDOB-based FCSCC transformed to Cartesian space

fluctuations of two curves in Fig. 4 (a), it can be seen that once the safety boundary is set near the expected contact force, the algorithm can effectively suppress the phenomena of force shock. Moreover, the comparison of the contact forces and compliance positions using NDOB-based force sensor-less FCSCC and sensor-based FCSCC approach shows that the replacement of force sensor with NDOB can ensure consistency in control performance. It can be seen from Fig. 5 that the proposed control quantities are adjusted once the constraints are not satisfied, proving the effectiveness of the two algorithms.

## VI. Experimental Results

In this section, the experimental tests are verified on a 6-degree-of-freedom industrial robot ER3A-C60 as shown in Fig. 6. Its setup block is shown in Fig. 5.


Fig. 6. The robot test platform with ER3A-C60 manipulator: A spring is used to generate contact force while the robot descends vertically.

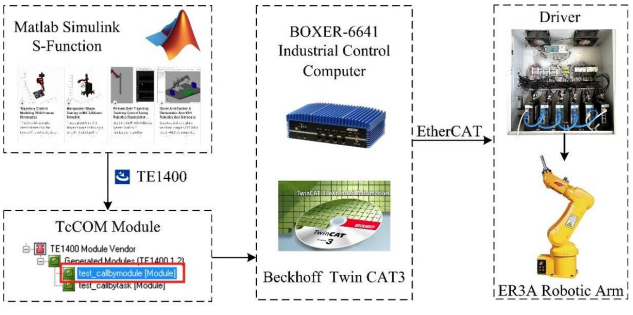


Fig. 7. The overall platform setup block.

The similar vertical moving task with strict force constraint in simulation part is considered where $F_{e\max}^c = 10N$. The stiffness of the spring is set as $K_{env}^{c_z} = 1000$, and the parameters of impedance controller are set as $M_d = 1\times I_{6\times6}$, $D_d = 35\times I_{6\times6}$, $K_d = 30\times I_{6\times6}$. The parameters of the constraints of FCCBF with/without force sensors are

$a=300, b=35$ and $a=237, b=85$, respectively. The experimental results are presented in Fig. 8 and Fig. 9.

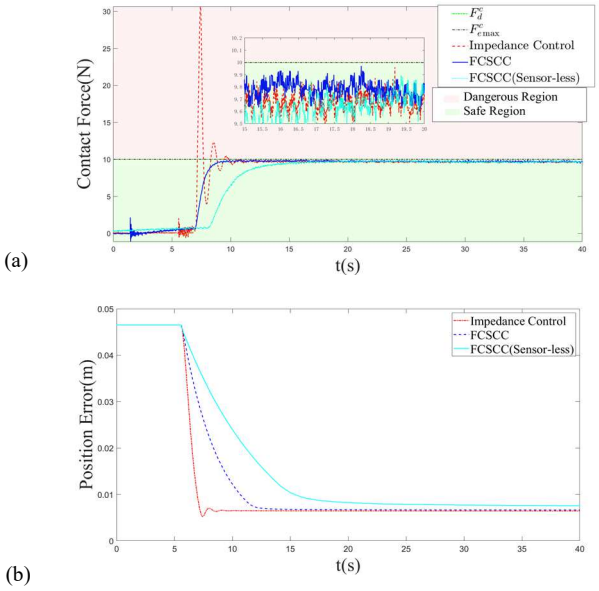


Fig.8. Experimental results: (a) trajectories of contact forces; (b) trajectories of compliance positions.

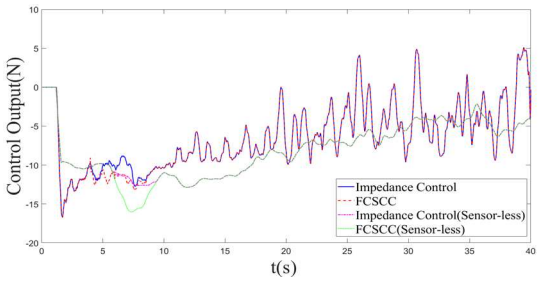


Fig.9. Experimental results of modified outputs $\gamma$ and baseline outputs $\gamma^d$ of sensor-based FCSCC and NDOB-based FCSCC in Cartesian space

From Fig. 8, the traditional impedance controller generates a huge contact force during the interaction, while the FCCBF-based approaches achieve the strict safety constraint and reduce the potential damage to the environment by suppressing the force fluctuations. In Fig. 9, the control inputs are illustrated, where the driving forces are adjusted once the FCCBF with/without sensors constraints are not satisfied.

## VII. CONCLUSION

This paper has investigated the safety and compliance problem of the contact force of the manipulator. Based on the design of FCCBF, a force-constrained safety compliance control strategy has been proposed by modifying the traditional impedance controller. Moreover, fully using the technique of nonlinear disturbance observer, a force sensor-less FCCBF approach has also been provided, where the contact force is treated as an external disturbance. Finally, the effectiveness in strict force constraint of the proposed methods have been verified by both simulations and experimental tests.

## REFERENCES


[1] Zhou, Y., Li, X., Yue, L., Gui, L., Sun, G., Jiang, X., & Liu, Y. H. (2019, July). Vision-based adaptive impedance control for robotic polishing. In 2019 Chinese Control Conference (CCC) (pp. 4560-4564). IEEE.

[2] Jo, J., Kim, S. K., Oh, Y., & Oh, S. R. (2011, November). Compliance control of a position controlled robotic hand using f/t sensors. In 2011 8th International Conference on Ubiquitous Robots and Ambient Intelligence (URAI) (pp. 446-450). IEEE.

[3] Xi, P., Ge, W., Zhang, S., Zhang, Z., & Zielinska, T. (2020, October). Finite Element Analysis of Series Elastic Actuator for Exoskeleton Robot Joint. In 2020 IEEE International Conference on Mechatronics and Automation (ICMA) (pp. 1935-1939). IEEE.

[4] Raibert, M. H. , & Craig, J. J. . (1981). Hybrid position/force control of manipulators. Asme Journal of Dynamic Systems Measurement & Control, 102(2), 126-133.

[5] Khatib, O. (1987). A unified approach for motion and force control of robot manipulators: The operational space formulation. IEEE Journal on Robotics and Automation, 3(1), 43-53.

[6] Hogan, N. (1984, June). Impedance control: An approach to manipulation. In 1984 American control conference (pp. 304-313). IEEE.

[7] Seraji, H. (1994, May). Adaptive admittance control: An approach to explicit force control in compliant motion. In Proceedings of the 1994 IEEE International Conference on Robotics and Automation (pp. 2705-2712). IEEE.

[8] Albu - Schäffer, A., Haddadin, S., Ott, C., Stemmer, A., Wimböck, T., & Hirzinger, G. (2007). The DLR lightweight robot: design and control concepts for robots in human environments. Industrial Robot: an international journal, 34(5), 376-385.

[9] Beretta, E., Nessi, F., Ferrigno, G., Di Meco, F., Perin, A., Bello, L., ... & De Momi, E. (2016). Enhanced torque - based impedance control to assist brain targeting during open - skull neurosurgery: a feasibility study. The International Journal of Medical Robotics and Computer Assisted Surgery, 12(3), 326-341.

[10] Kitazawa, T., Kurisu, M., & Takemasa, S. (2017, December). Impedance control of a mobile robot with dual arms for a tumbling operation. In 2017 11th Asian Control Conference (ASCC) (pp. 25-30). IEEE.

[11] Duan, J. , Gan, Y. , Chen, M. , & Dai, X. . (2018). Adaptive variable impedance control for dynamic contact force tracking in uncertain environment. Robotics and Autonomous Systems. 102(2), 54-65.

[12] Wang, X., Lyu, Z., & Dong, Y. (2022, July). A Unified Approach for Safety Critical Control Problem via Output Regulation Theory and Barrier Function. In 2022 41st Chinese Control Conference (CCC) (pp. 833-837). IEEE.

[13] Zhu, Z., Chai, Y., Song, Z., & Huang, P. (2021, December). A New Safety Criterion for Dynamics Systems by Barrier Function based on Forward Invariant Set. In 2021 CAA Symposium on Fault Detection, Supervision, and Safety for Technical Processes (SAFEPROCESS) (pp. 1-6). IEEE.

[14] Ames, A. D., Coogan, S., Egerstedt, M., Notomista, G., Sreenath, K., & Tabuada, P. (2019, June). Control barrier functions: Theory and applications. In 2019 18th European control conference (ECC) (pp. 3420-3431). IEEE.

[15] Wang, L., Ames, A. D., & Egerstedt, M. (2017). Safety barrier certificates for collisions-free multirobot systems. IEEE Transactions on Robotics, 33(3), 661-674.

[16] Ducaju, J. M. S., Olofsson, B., Robertsson, A., & Johansson, R. (2022, August). Robot Cartesian compliance variation for safe kinesthetic teaching using safety control barrier functions. In 2022 IEEE 18th International Conference on Automation Science and Engineering (CASE) (pp. 2259-2266). IEEE.

[17] Adinehvand, M., Lai, C. Y. and Hoseinnezhad, R. (2021). Barrier-Lyapunov -Function-Based Backstepping Adaptive Hybrid Force/Position Control for Manipulator with Force and Position Constraints. American Control Conference (ACC) (pp. 2266-2271). IEEE.

[18] Nguyen, Q. , & Sreenath, K. . (2016). Exponential control barrier functions for enforcing high relative-degree safety-critical constraints. American Control Conference (ACC) (pp. 322–328). IEEE.

[19] Chen, W. H. , & Ballance, D. J. . (2000). A nonlinear disturbance observer for robotic manipulators. IEEE Transactions on Industrial Electronics, 47(4), 932-938.

[20] Yousefizadeh, S. , & Bak, T. . (2019). Nonlinear Disturbance Observer for External Force Estimation in a Cooperative Robot. 2019 19th International Conference on Advanced Robotics (ICAR) (pp. 220-226). IEEE.